

## Direct Observation of Excitonic Rabi Oscillations in Semiconductors

A. Schülzgen,<sup>1,\*</sup> R. Binder,<sup>1</sup> M. E. Donovan,<sup>1</sup> M. Lindberg,<sup>2</sup> K. Wundke,<sup>1</sup> H. M. Gibbs,<sup>1</sup>  
G. Khitrova,<sup>1</sup> and N. Peyghambarian<sup>1</sup>

<sup>1</sup>*Optical Sciences Center, University of Arizona, Tucson, Arizona 85721*

<sup>2</sup>*Institutionen för Fysik, Åbo Akademi, Porthansgatan 3, 20500 Åbo, Finland*

(Received 8 December 1998)

We observe multiple excitonic optical Rabi oscillations in a semiconductor quantum well. Up to eight oscillation periods of the heavy-hole exciton density on a subpicosecond time scale are observed. An approximate linear dependence of the oscillation frequency on the light field amplitude is established. The experiment is based on a two-color detection scheme which allows for the observation of the heavy-hole exciton density via transmission changes at the light-hole exciton. The observations are in good agreement with theoretical computations based on multiband semiconductor Bloch equations. [S0031-9007(99)08665-2]

PACS numbers: 71.35.Cc, 42.50.Md, 78.20.-e, 78.47.+p

Optical Rabi oscillations are among the most fundamental examples of coherent nonlinear light-matter interactions. In atomic and molecular two-level systems, optical Rabi oscillations are well established [1]. Exposed to a strong stationary light field, the electron population oscillates between the lower and upper states with the Rabi frequency that is proportional to the dipole moment and the light field. Early experiments in atoms evolved from indirect observations which utilized the fact that Rabi oscillations yield certain signatures in the temporal reshaping of transmitted light pulses [2,3], to rather direct observations of multiple oscillations [4,5]. In the latter, the fluorescence signal was used to measure oscillations as a function of pulse area (i.e., time-integrated Rabi frequency). These experiments established the correspondence in principle between optical Rabi oscillations and the original Rabi oscillations of magnetic two-level systems [6] and proved the applicability of the theory of two-level atoms in nonlinear optics.

During the last decade, attempts have been made to establish the correspondence and to identify principal differences between two-level atoms and excitons in semiconductors. In spite of the fact that coherent nonlinear optical effects in semiconductors require ultrafast experimental techniques because of short dephasing times, many analogies have been successfully investigated, such as the excitonic optical Stark effect, free induction decay, and photon echoes in four-wave mixing experiments [7]. As for excitonic Rabi oscillations, indications for their existence have already been obtained from measurements of temporal pulse reshaping [8–10]. These nonlinear light propagation effects are, however, only very indirect indications of possible Rabi oscillations. This is particularly true for optically thick samples, where the backreaction of the medium can no longer be neglected and self-induced transparency replaces Rabi oscillations. A more direct observation of interband density oscillations due to optical fields with center frequencies far above the exciton resonance was

reported in [11,12] but excitonic Rabi oscillations do not occur since no bound electron-hole pairs (excitons) are excited.

In this Letter we present experimental results along with theoretical calculations for excitonic optical Rabi oscillations in semiconductor quantum wells. The observations are based on a direct time-resolved measurement of the exciton density utilizing a two-color pump-and-probe scheme similar to the one used in [11]. An important aspect of our measurement is that we are able not only to observe multiple oscillations but also to determine the dependence of the excitonic Rabi oscillation frequency upon pulse intensity. This permits a detailed comparison of the observations with theoretical computations and plays a significant role in establishing the desired correspondence with atomic systems.

Figure 1 shows the experimental scheme. The linear transmission spectrum of the  $\text{In}_{0.1}\text{Ga}_{0.9}\text{As}/\text{GaAs}$  multiple quantum well sample with 20 periods and 8 nm well width is given in Fig. 1(a). This sample is characterized by small inhomogeneous line broadening and an intentionally large strain induced splitting of 18.5 nm between  $1s$  heavy-hole (hh) and  $1s$  light-hole (lh) exciton absorption resonances. Independently tunable pump and probe pulses are generated by an amplified Ti:Sapphire laser system that pumps two optical parametric amplifiers at a 1 kHz repetition rate. Pulse shaping and polarization elements result in 770 fs  $\sigma^-$  circularly polarized pump pulses with a narrow spectrum resonant to the  $1s$  hh exciton transition, and 150 fs  $\sigma^+$  probe pulses that are centered at the  $1s$  lh exciton resonance [see Fig. 1(b)]. The pulses are focused down to 200 and 100  $\mu\text{m}$  for the pump and the probe, respectively, on the sample that is held at 5 K. The zero delay is measured by cross correlation in a BBO (beta barium borate) crystal, and the time jitter between pump and probe is found to be less than 20 fs. An optical multichannel analyzer has been used to detect the differential transmission signal (DTS) as a function of pump-probe delay.

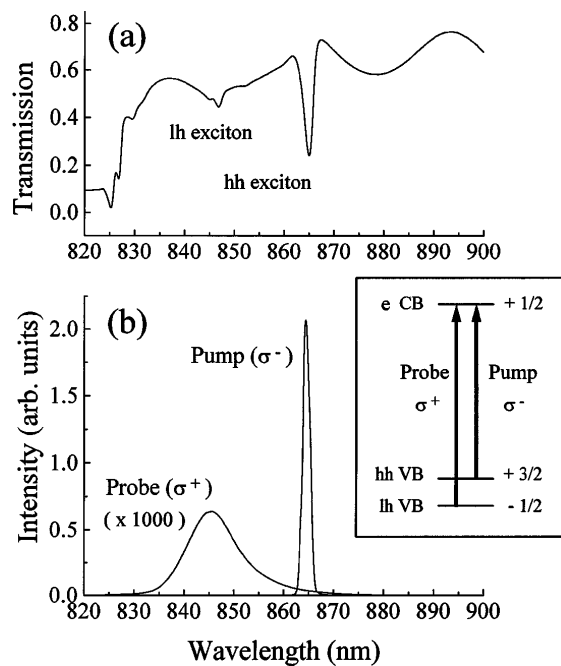


FIG. 1. (a) Transmission spectrum of the  $\text{In}_{0.1}\text{Ga}_{0.9}\text{As}/\text{GaAs}$  multiple quantum well at 5 K. (b) Spectra of the pump and probe pulse. Inset: Schematic illustration of the spectral pump-probe configuration. The numbers indicate the angular momentum of the states close to the center of the Brillouin zone. CB: conduction band, VB: valence band. Transitions involving the states with opposite angular momentum are out of resonance, and hence not shown.

While the long pump pulse drives the Rabi oscillations in the population, the much shorter probe pulse gates the transmission changes. As illustrated schematically in the inset of Fig. 1, the polarization of pump-and-probe pulses and the large hh-lh valence band splitting allow us to monitor separately the dynamics of the  $s = +\frac{1}{2}$  electron population in the conduction band. A direct excitation of  $s = -\frac{1}{2}$  electrons is strongly suppressed due to both the narrow spectrum of the pump pulse and the large valence band splitting. In contrast to previous work [8,11], where 100 fs pulses were used, our long pump pulses have large (several  $\pi$ ) areas at relatively small field intensities. Correspondingly, the induced carrier densities are quite low, resulting in weak excitation-induced dephasing and, accordingly, long time windows for the observation of coherent dynamics.

Figure 2(a) shows the DTS at the position of the lh exciton resonance for a pump pulse energy flux of  $16 \text{ nJ}/\text{cm}^2$ . One can clearly resolve in time a sequence of eight Rabi oscillations during the interaction between the pump pulse and the semiconductor material. One can also see the time dependence of the period, with longer periods at the leading and trailing edges of the pump pulse.

The theoretical prediction of excitonic Rabi oscillations was made in [13] where the most basic form of the two-band semiconductor Bloch equations (SBE) was

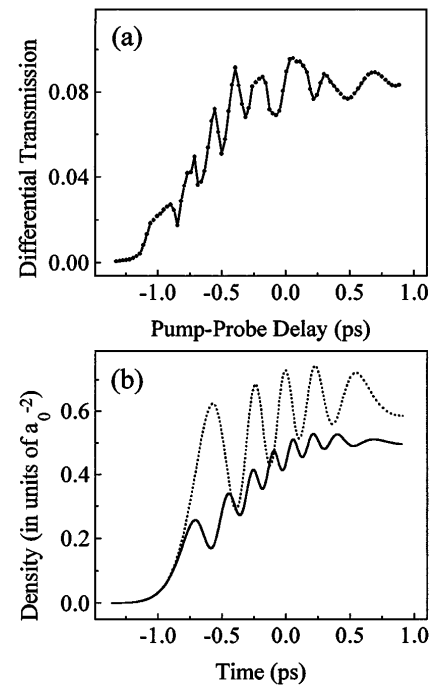


FIG. 2. (a) Differential transmission signal (DTS) vs pump-probe delay measured at the lh exciton absorption resonance. (b) Theoretical calculation of the  $s = +\frac{1}{2}$  electron density dynamics for a 770 fs Gaussian-shaped pulse with (solid line) and without (dotted line) nonlinear Coulomb-renormalization terms ( $a_0 = 13.5 \text{ nm}$ ).

used. There it was found that the Coulomb interaction allows for oscillations in the excitonic density, in spite of the facts that (i) the underlying band-to-band transitions in the one-particle picture form a continuous set with momentum-dependent detuning, (ii) in contrast to a two-level system there is no strict upper limit for the excitation density, and (iii) the light-induced charge carriers yield a time-dependent renormalization of the transition energy and the Rabi frequency. A detailed study of the underlying one-particle distribution functions shows that, at low intensities, the distribution functions are proportional to excitonic envelope functions. Because of fermionic Pauli blocking, the one-particle distributions deviate significantly from excitonic envelope functions at high intensities [14]. The theoretical description of the nonlinear coherent excitation of semiconductors can also be based on appropriate extensions of the SBE [12,14] that include a microscopic description of carrier scattering and dephasing processes.

In this Letter, we use the basic Hartree-Fock form of the SBE, extended to include two hh, two lh, and two conduction bands with input parameters corresponding to the experiment, and compare the predictions of the SBE with the experimental data. In this formulation one solves equations of motion for the momentum-resolved interband polarizations  $P_{sj}(k)$ , where  $s$  and  $j$  are the conduction- and valence-band indices, and for the carrier distribution

functions for electrons ( $f_{ss'}$ ) and holes ( $f_{jj'}$ ). The equations are given in [15]. These equations contain the appropriate optical selection rules via the dipole energies  $\mu_{sj}E(t)$  [where  $\mu_{sj}$  is the dipole matrix element at the zone center and  $E(t)$  is the electric field], Pauli blocking terms, and Coulomb interaction terms. The latter include linear exciton effects and the nonlinear renormalization of the one-particle energies and of the effective Rabi frequency energy within the mean-field [Hartree-Fock (HF)] approximation.

To simulate the experiment quantitatively, we have to know several parameters that characterize our specific experiment. We have determined the value for  $\mu_{sj}$  by computing the linear absorption spectrum and adjusting the numerical value for the absorption at frequencies just above the hh band gap to coincide with the experimental value. This yields  $\mu_{cv}/e = 5.75 \text{ \AA}$  (here,  $e$  is the electron charge in vacuum). To relate the measured light intensity outside the sample to its value inside the sample (the latter is the one used in the calculations) we use the refractive index  $n = 3.6$  and a corresponding normal-incidence reflection loss of 32%. The other parameters needed in the microscopic calculation are the hh-lh splitting ( $\Delta_{\text{hh-lh}} = 30 \text{ meV}$ ), the Luttinger parameters ( $\gamma_1 = 6.85$ ,  $\gamma_2 = 2.1$ ,  $\gamma_3 = 2.9$ ), the effective electron mass ( $m_e = 0.067$ ), the background dielectric constant entering the Coulomb potential ( $\epsilon_0 = 12.7$ ), the quantum well thickness entering the form factor of the Coulomb potential ( $L = 8 \text{ nm}$ ), and the dephasing time ( $T_2 = 526 \text{ fs}$ ). Based on the experimental fact of small excitation induced resonance broadening the dephasing time was chosen to coincide with the inverse width of the hh exciton absorption resonance that represents a lower limit for the dephasing time. Since the calculated Rabi oscillation period does not depend strongly on the exact value of the dephasing time [13] the conclusions discussed below do not depend on the specific value of  $T_2$ .

Figure 2(b) shows the calculated electron density in the  $s = +\frac{1}{2}$  conduction band induced by a 770 fs Gaussian-shaped pulse with center frequency at the hh exciton and a pulse energy flux outside the sample of  $16 \text{ nJ/cm}^2$ . This corresponds to an unrenormalized pulse area of  $10.3\pi$ , as shown by the dotted curve in Fig. 2(b) computed omitting all nonlinear Coulomb-renormalization terms (i.e., products of polarization and distribution functions). Results including these nonlinear terms, solid curve in Fig. 2(b), agree well with the experimental data as shown by the same number of oscillations. This again illustrates the important prediction [13] that the effective dipole moment is increased by excitonic many-body Coulomb effects.

We have also performed a detailed study of the intensity dependence of the oscillation period by varying the pump pulse energy flux while the other pulse parameters remain unchanged. In Fig. 3 we plot the measured and calculated oscillation frequency for different pump energy fluxes. The experimental data (open symbols) are

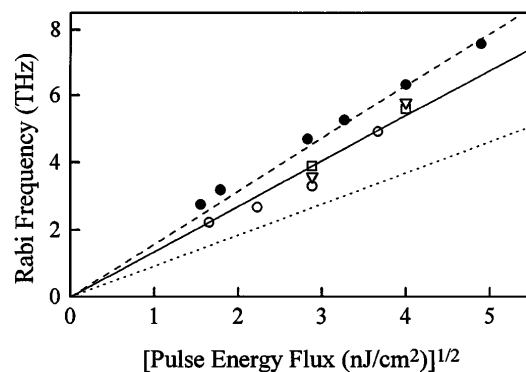


FIG. 3. Measured (open symbols) and calculated (filled symbols) Rabi oscillation frequency vs square root of the pulse energy flux. The lines illustrate the approximate linear dependence. For comparison the dotted line shows the computed dependence omitting the nonlinear Coulomb-renormalization terms.

extracted from the respective DTS vs time delay plots (see Fig. 2) by measuring the time separation between the DTS maxima (we averaged over the two fastest oscillations) and inverting this number. Different symbols correspond to different measurement series, illustrating the reproducibility of our results. Within our range of intensities we find an approximate square-root dependence of the oscillation frequency on pulse energy flux that corresponds to an almost linear relation between the frequency of the Rabi oscillation and the electric field amplitude. The filled circles show the corresponding theoretical results extracted in the same way from the calculated electron densities. Whereas in atoms the Rabi frequency is simply given by  $\Omega_R(t) = \mu E(t)/\hbar$ , the effective Rabi frequency in semiconductors is  $\Omega_R(t) = \mu_{sj}E(t)/\hbar + \text{Coulomb terms}$ , i.e., it is renormalized by interaction effects. Within the HF theory, the Coulomb renormalization has been found to be significant [13] [cf. Fig. 2(b)]. On the other hand, Fig. 3 shows that this renormalization does not alter the basic linear dependence on field amplitude very much, at least in the intensity regime under consideration. Figure 3 also suggests that calculations beyond HF can be expected to yield an intensity dependence in between the HF result and the results where nonlinear Coulomb terms are omitted, and, thus, to yield even better agreement with the experiment than already obtained here.

In conclusion, we present the first direct measurement of multiple-cycle excitonic Rabi oscillations in semiconductors and observation of an approximate linear dependence of the oscillation frequency upon the electric field amplitude. We also find surprisingly good agreement of the experimental observations with the predictions based on the multiband semiconductor Bloch equations evaluated in the Hartree-Fock approximation.

We would like to acknowledge financial support from ARO, JSOP, AFOSR, and COEDIP (University of Arizona), and CPU time at the CCIT, University of Arizona.

M.L. appreciates the travel grant by Svenska Tekniska Vetenskapsakademien i Finland.

---

\*Electronic address: axel@u.arizona.edu

- [1] L. Allen and J.H. Eberly, *Optical Resonance and Two-Level Atoms* (Wiley, New York, 1975).
- [2] G.B. Hocker and C.L. Tang, Phys. Rev. Lett. **21**, 591 (1968).
- [3] P.W. Hoff, H.A. Haus, and T.J. Bridges, Phys. Rev. Lett. **25**, 82 (1970).
- [4] H.M. Gibbs, Phys. Rev. A **8**, 446 (1973).
- [5] Y.S. Bai, A.G. Yodh, and T.W. Mossberg, Phys. Rev. Lett. **55**, 1277 (1985).
- [6] I.I. Rabi, Phys. Rev. **51**, 652 (1937); I.I. Rabi, S. Milliman, P. Kusch, and J.R. Zacharias, Phys. Rev. **55**, 526 (1939).
- [7] J. Shah, *Ultrafast Spectroscopy of Semiconductors and Semiconductor nanostructures* (Springer, Berlin, 1996), and references therein.
- [8] S.T. Cundiff, A. Knorr, J. Feldmann, S.W. Koch, E.O. Goebel, and H. Nickel, Phys. Rev. Lett. **73**, 1178 (1994).
- [9] H. Giessen, A. Knorr, S. Haas, S.W. Koch, S. Linden, J. Kuhl, M. Hetterich, M. Grun, and C. Klingshirn, Phys. Rev. Lett. **81**, 4260 (1998).
- [10] A theoretical analysis of the configuration used in [9] is given in I. Talanina, D. Burak, R. Binder, H. Giessen, and N. Peyghambarian, Phys. Rev. E **58**, 1074 (1998).
- [11] C. Fürst, A. Leitenstorfer, A. Nutsch, G. Tränkle, and A. Zrenner, Phys. Status Solidi (b) **204**, 20 (1997).
- [12] A theoretical analysis of the configuration used in [11] is given in L. Banyai, Q.T. Vu, B. Mieck, and H. Haug, Phys. Rev. Lett. **81**, 882 (1998).
- [13] R. Binder, S.W. Koch, M. Lindberg, and N. Peyghambarian, Phys. Rev. Lett. **65**, 899 (1990).
- [14] R. Binder and S.W. Koch, Prog. Quantum Electron. **19**, 307 (1995).
- [15] R. Binder and M. Lindberg, Phys. Rev. Lett. **81**, 1477 (1998).